Multiple Charge Density Waves and Superconductivity Nucleation at Antiphase Domain Walls in the Nematic Pnictide $Ba_{1-x}Sr_xNi_2As_2$

Sangjun Lee,[1] John Collini,[2] Stella X.-L. Sun,[1] Matteo Mitrano,[1] Xuefei Guo,[1] Chris Eckberg,[2] Johnpierre Paglione,[2,3] Eduardo Fradkin,[1,4] and Peter Abbamonte[1,*]

[1]*Department of Physics and Materials Research Laboratory, University of Illinois, Urbana, Illinois 61801, USA*
[2]*Maryland Quantum Materials Center, Department of Physics, University of Maryland, College Park, Maryland 20742, USA*
[3]*Canadian Institute for Advanced Research, Toronto, Ontario M5G 1Z8, Canada*
[4]*Institute of Condensed Matter Theory, University of Illinois, Urbana, Illinois 61801, USA*

(Received 6 February 2021; accepted 21 May 2021; published 6 July 2021)

How superconductivity interacts with charge or nematic order is one of the great unresolved issues at the center of research in quantum materials. $Ba_{1-x}Sr_xNi_2As_2$ (BSNA) is a charge ordered pnictide superconductor recently shown to exhibit a sixfold enhancement of superconductivity due to nematic fluctuations near a quantum phase transition (at $x_c = 0.7$) [1]. The superconductivity is, however, anomalous, with the resistive transition for $0.4 < x < x_c$ occurring at a higher temperature than the specific heat anomaly. Using x-ray scattering, we discovered a new charge density wave (CDW) in BSNA in this composition range. The CDW is commensurate with a period of two lattice parameters, and is distinct from the two CDWs previously reported in this material [1,2]. We argue that the anomalous transport behavior arises from heterogeneous superconductivity nucleating at antiphase domain walls in this CDW. We also present new data on the incommensurate CDW, previously identified as being unidirectional [2], showing that it is a rotationally symmetric "4Q" state with C_4 symmetry. Our study establishes BSNA as a rare material containing three distinct CDWs, and an exciting test bed for studying coupling between CDW, nematic, and SC orders.

DOI: 10.1103/PhysRevLett.127.027602

One of the perennial questions in quantum materials is to what extent superconductivity (SC) may be enhanced by coupling to other Fermi surface instabilities, such as charge density wave (CDW), spin density wave (SDW), or nematic orders. This issue has been investigated most widely in cuprate and iron-based superconductors [3–6]. While spin fluctuations are considered a primary ingredient in Cooper pairing in both materials, the CDW in cuprates [7–9] and nematic fluctuations in iron-based materials [10,11] are pervasive and suggest a close interrelation between SC and these other electronic instabilities. The importance of such orderings for SC is still unclear, so there is a great need for new materials that can provide fresh insight.

$Ba_{1-x}Sr_xNi_2As_2$ is a nickel-based pnictide superconductor that is an ideal system to investigate the relationship between charge instabilities and SC. We recently showed that $BaNi_2As_2$ exhibits two distinct CDW instabilities that arise sequentially on lowering temperature [2]. In the tetragonal phase, an incommensurate CDW (IC-CDW), previously identified as unidirectional, forms along the in-plane H axis with wave vector $q = 0.28$. Upon cooling across the structural transition to the triclinic phase, the IC-CDW is replaced by the second CDW, which we denote C-CDW-1, which is commensurate with $q = 1/3$. This CDW arises via a lock-in transition from an incipient, slightly incommensurate CDW with $q \sim 0.31$ [2].

When $BaNi_2As_2$ is substituted with Sr or Co, the triclinic phase that hosts C-CDW-1 is suppressed and a SC dome emerges [1,2,12], suggesting C-CDW-1 plays a similar role to antiferromagnetism in chemically substituted $BaFe_2As_2$. Further, full suppression of the CDW by Sr substitution, which occurs at the critical composition $x_c = 0.7$, results in a quantum phase transition (QPT) characterized by nematic fluctuations that drive a sixfold enhancement of the superconducting T_c [1,13]. $Ba_{1-x}Sr_xNi_2As_2$ is therefore an exciting new system in which the interaction between SC, CDW, and nematic order can be studied in detail.

Recent studies revealed two peculiar properties of $Ba_{1-x}Sr_xNi_2As_2$ that are not fully understood [1,2]. First, for the composition range of $0.4 < x < x_c$, the SC transition in transport measurements is broadened and occurs at a higher temperature than the specific heat anomaly [1]. Why the resistive and thermodynamic transitions should be split in this manner is not known. Second, the IC-CDW was identified in Ref. [1] as a lattice-driven instability, without electronic character, since it shows no precursor response in the nematic susceptibility. However, it was also observed that the elastoresistance becomes hysteretic whenever the IC-CDW is present, suggesting the two phases are coupled. These two observations are seemingly contradictory, since a purely structural phase transition should not influence the nematic response in

this way. The nature of the interaction between the IC-CDW and the nematic phase remains unclear.

Here, using x-ray scattering, we present the discovery of a *third* CDW in $Ba_{1-x}Sr_xNi_2As_2$, which we denote C-CDW-2, in the composition range $0.4 < x < x_c$, where $x_c = 0.7$. This CDW is commensurate with a period of two lattice parameters (period-2). While a CDW with a generic wave vector has a complex order parameter [14], the period-2 CDW state is special in that its order parameter is real. We will show below that competing (weaker) SC state can be nucleated on topological defects of a period-2 CDW such as domain walls. The implication is that the phase at $0.4 < x < x_c$ may be a heterogeneous state in which SC resides at the topological defects of the CDW order.

Further, we report a wider x-ray momentum survey showing that the IC-CDW phase is in fact bidirectional with 90° rotational symmetry. We observed additional satellite reflections demonstrating a coherent "4Q" state with C_4 symmetry that does not break the rotational symmetry of the underlying tetragonal lattice. This observation explains the absence of a precursor nematic response in elastoresistivity measurements [1], and suggests this CDW could be electronic and strongly coupled to the nematic order.

Single crystals of $Ba_{1-x}Sr_xNi_2As_2$ with $x = 0$, 0.27, 0.42, 0.47, 0.65, and 0.73 were measured in this study. Three-dimensional x-ray surveys of momentum space were obtained using a Mo K_α (17.4 keV) microspot x-ray source and a Mar345 image plate detector by sweeping crystals through an angular range of 20°. All temperature evolution measurements in this study are conducted while warming the samples starting from low temperature (see Supplemental Material for experimental details [15]).

The parent compound, $BaNi_2As_2$, has tetragonal $I4/mmm$ symmetry at room temperature and undergoes a phase transition to triclinic $P\bar{1}$ at $T_s = 136$ K [2,26]. This transition is observed in x-ray measurements as a splitting of the tetragonal reflections into four peaks due to the formation of triclinic twin domains [2,26] (see Supplemental Material for more details [15]). Measurements in the triclinic phase were indexed by selecting a single subset of these four reflections, emphasizing scattering from a single domain. Figures 1(a) and 1(b) show the conventional unit cells and the BZ boundaries in the tetragonal and triclinic phases. Throughout this Letter, we use $(H, K, L)_{\text{tet}}$ and $(H, K, L)_{\text{tri}}$ to denote indices in the tetragonal and triclinic unit cells, respectively.

Here, we find that when $BaNi_2As_2$ is substituted with Sr, the triclinic transition as seen with x rays initially increases in temperature, reaching a maximum $T_s = 141$ K at $x = 0.27$. Further substitution decreases T_s until, at $x = 0.73$, the structure transition is no longer observed, indicating a quantum phase transition at $x_c \sim 0.7$, consistent with conclusions from transport experiments [1]. In Fig. 5 we compare our results to the transport phase diagram of $Ba_{1-x}Sr_xNi_2As_2$. The triclinic transition

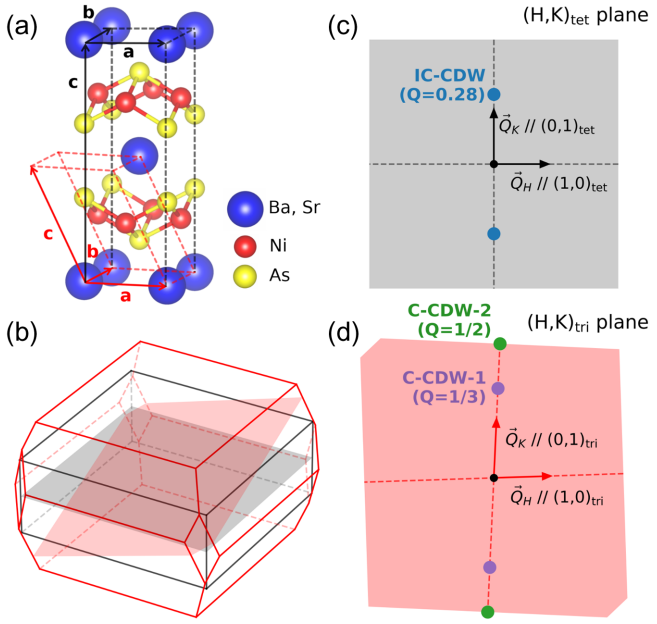

FIG. 1. (a) The crystal structure of $Ba_{1-x}Sr_xNi_2As_2$ and the unit cells of tetragonal (black lines) and triclinic phases (red lines). (b) The BZ boundaries of tetragonal (black lines) and triclinic (red lines) phases. The planes colored in black and red represent H-K planes in the tetragonal and triclinic phases, respectively. (c),(d) The H-K planes of tetragonal and triclinic phases, respectively, showing the location of three CDWs in momentum space in each phase.

determined by x-ray scattering while warming (purple line) is slightly higher in temperature than the cooling transition determined by transport (black dashed line) [1], demonstrating the first order nature of the transition. Nevertheless, we see no evidence for coexistence of tetragonal and triclinic phases, unlike Co-substituted compounds, $Ba(Ni_{1-x}Co_x)_2As_2$, in which an extended region of coexistence occurs [2].

The primary result of this study is the discovery in the composition range $0.4 < x < x_c$ of a third CDW, which we denote C-CDW-2. This CDW is distinct from the IC-CDW and C-CDW-1 phases reported previously [1,2]. Figure 2 shows x-ray measurements of the sample with $x = 0.42$, in which all three CDWs are observed sequentially upon cooling. The IC-CDW forms at the highest temperature, at $T_{\text{IC}} = 132.5 \pm 2.5$ K. Its wave vector, shown in the (1,1,5) BZ in Figs. 2(a),2(d), is $q = (0, 0.28, 0)_{\text{tet}}$, which is the same reported in the parent compound [2]. No corresponding reflection was observed at $(0.28, 0, 0)_{\text{tet}}$ in this zone, which previously led us to the conclusion that the IC-CDW is unidirectional [2]. Below, we present data revising this conclusion. In Co-substituted materials, the IC-CDW was only observed in the parent compound and disappeared at Co content of 0.07 [2]. We note that the IC-CDW could be present at intermediate Co substitution in $Ba(Ni_{1-x}Co_x)_2As_2$, just as it persists up to $x = 0.47$ in $Ba_{1-x}Sr_xNi_2As_2$.

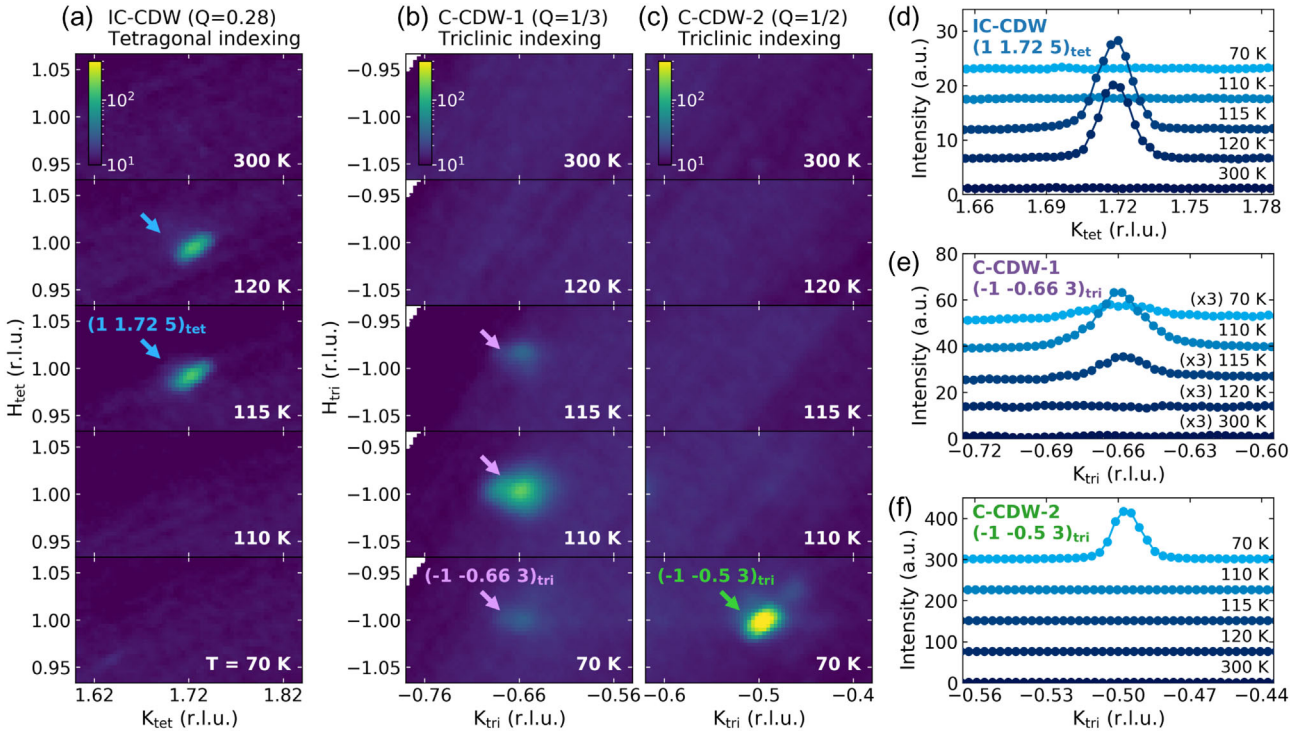

FIG. 2. Three distinct CDWs in $Ba_{0.58}Sr_{0.42}Ni_2As_2$. (a),(b),(c) H-K maps of IC-CDW, C-CDW-1, and C-CDW-2, respectively, at a selection of temperatures. (d), (e), (f) Line momentum scans of the CDW reflections shown in (a),(b), and (c), respectively, along the corresponding modulation direction.

Upon further cooling, the IC-CDW is replaced by C-CDW-1 at $T_{C1} = 117.5 \pm 2.5$ K [Figs. 2(b), 2(e)], which coincides with the triclinic transition. Its wave vector is $q = (0, 1/3, 0)_{\text{tri}}$, which is commensurate with a period of three lattice parameters. As in the case of IC-CDW, no $(1/3, 0, 0)_{\text{tri}}$ peak was observed. This CDW is also observed in Co-substituted compounds, where it exhibits a lock-in effect [2]. However, we observe no lock-in effect in Sr-substituted materials.

A third, previously unobserved CDW, which we call C-CDW-2, appears at lower temperature, $T_{C2} = 95 \pm 5$ K [Figs. 2(c), 2(f)]. Its wave vector, $q = (0, 1/2, 0)_{\text{tri}}$ is commensurate with a period of two lattice parameters. Again, no corresponding peak was observed at $q = (1/2, 0, 0)_{\text{tri}}$. When C-CDW-2 forms, the magnitude of the triclinic distortion increases [Fig. S1(c) in Supplemental Material [15]] while the C-CDW-1 order parameter is suppressed [Fig. 4(c)]. This indicates that C-CDW-2 competes with C-CDW-1, but has a cooperative relationship with the triclinic phase itself. None of these effects were observed in $Ba(Ni_{1-x}Co_x)_2As_2$, indicating that C-CDW-2 is specific to the current material and does not arise with Co substitution. We summarize the momentum space locations of all three CDWs in Figs. 1(b)–1(d). We emphasize that these three CDWs reside in very different locations in momentum space, as illustrated in Fig. 1; the difference between the three CDW wave vectors is not merely due to a change of indexing coordinates.

We now discuss the rotational symmetry of the three CDWs. The satellite reflections in all three phases appear in only one direction in a given BZ, which would normally be interpreted as evidence that all three CDWs are unidirectional. This is unsurprising for C-CDW-1 and C-CDW-2 since they reside in the triclinic phase in which C_4 (rotational) symmetry is broken by the underlying lattice. However, it is puzzling that IC-CDW should also be unidirectional, since it resides in the tetragonal phase where C_4 symmetry is preserved. Our claim that IC-CDW is unidirectional [2] led the authors of Ref. [1] to conclude that the IC-CDW is a purely structural phase transition, uncoupled to the valence electron system, since they observed no precursor response in the nematic susceptibility expected of an electronic phase with broken rotational symmetry.

We reexamined this issue by performing a wide, three-dimensional x-ray survey of a 20° wedge of momentum space, analyzing where CDW satellites reside in multiple BZs. We found that the C-CDW-1 and C-CDW-2 show the same unidirectionality in all zones observed (see Supplemental Material [15]), affirming that these triclinic CDWs are unidirectional as claimed [2]. However, the IC-CDW exhibits the more complicated pattern shown in

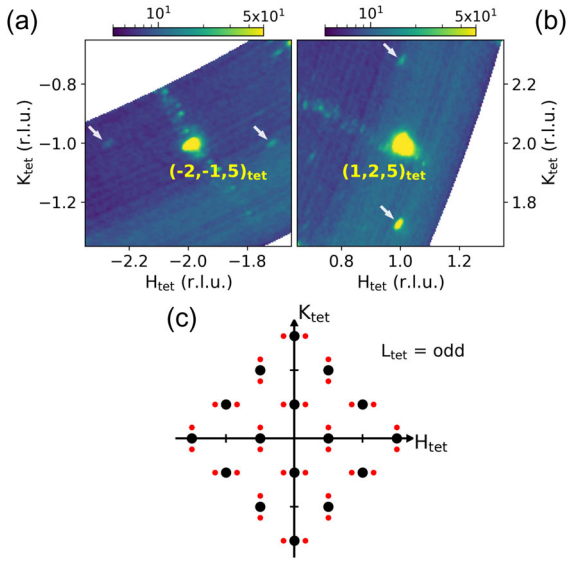

FIG. 3. (a) H-K map around $(-2,-1,5)_{\mathrm{tet}}$ showing the IC-CDW satellites at $(\pm 0.28,0,0)_{\mathrm{tet}}$. The satellites are absent at $(0,\pm 0.28,0)_{\mathrm{tet}}$. (b) H-K map around $(1,2,5)_{\mathrm{tet}}$ showing the satellites at $(0,\pm 0.28,0)_{\mathrm{tet}}$. The satellites are absent at $(\pm 0.28,0,0)_{\mathrm{tet}}$. (c) Illustration of the symmetry pattern of IC-CDW in H-K plane at odd-numbered L. Black dots represent Bragg peak locations, and red dots represent IC-CDW peak locations.

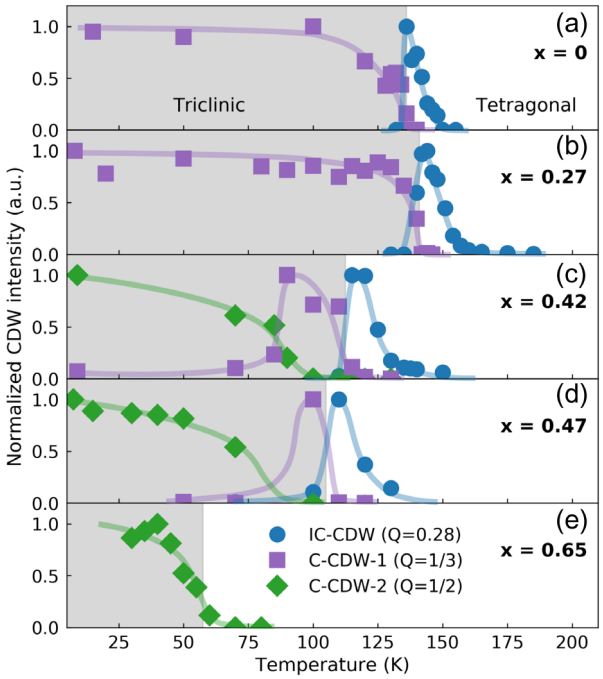

FIG. 4. Warming temperature dependence of the integrated intensities of the IC-CDW (blue circles), C-CDW-1 (purple squares), and C-CDW-2 (green diamonds) reflections. The Sr composition, x, is shown in each panel. The shaded region represents the temperature range of the triclinic phase. Each curve is scaled to the maximum CDW intensity at low temperature. The solid lines are guides to the eye.

Fig. 3. While any given BZ has only two satellites, their orientation is different in different BZs. The overall pattern is invariant under 90° rotations around the origin, and therefore exhibits the same C_4 symmetry as the underlying tetragonal lattice. We conclude that the IC-CDW is not unidirectional, but is a coherent $4Q$ state in which two reflections in each BZ are extinguished by some additional symmetry. This result implies that IC-CDW may be electronic in origin after all, and may couple strongly to the nematic order.

Figure 4 summarizes the behavior of the three CDWs over the full range of Sr composition investigated. The IC-CDW is present from $x = 0$ to 0.47. The C-CDW-2 phase is first observed at $x = 0.42$, where it replaces C-CDW-1 in the triclinic phase, and persists up to $x = 0.65$ [27]. At $x = 0.73$, no CDW transition is observed. No two CDWs are ever optimized at the same composition or temperature, indicating that the three phases likely compete with one another.

A summary phase diagram of $Ba_{1-x}Sr_xNi_2As_2$ is presented in Fig. 5. The anomalous superconducting phase at $0.4 < x < x_c$, in which transport and thermodynamic signatures occur at different temperatures [1], resides entirely within the C-CDW-2 phase. By contrast, at $x > x_c$ when no CDW is present, the superconducting signatures are normal. This implies that the peculiar superconducting state reported in Ref. [1] is connected to the presence of C-CDW-2.

A period-2 CDW competing with superconductivity is prone to developing a heterogeneous mixed state. The order parameter of period-2 CDW is real, since its phase can only be either 0 or π, i.e., the order parameter itself is either ψ or $-\psi$, where ψ is a real number [15]. A CDW is highly sensitive to disorder [28], trace amounts of which can lead to the formation of domain walls with a π phase shift, across which the order parameter changes sign and, thus, vanishes. Since the CDW is suppressed at the domain walls, these locations are favorable for competing superconductivity to emerge, resulting in a heterogeneous or filamentary superconducting state. In Supplemental Material Sec. VI [15], we present a phenomenological theory of this situation. We consider the simplest form of the Landau-Ginzburg free energy with competing CDW and SC orders as given by Eq. (2) in Supplemental Material [15], and obtain solutions in the presence of a domain wall. The corresponding Landau-Ginzburg equation [Eq. (12) in Supplemental Material [15]] has a nontrivial domain wall solution in which the CDW order parameter changes sign. At the location of the topological defect, the SC order parameter is nonzero, and decays exponentially away from the domain wall. We therefore identify this unusual SC state as a heterogeneous state in which SC is locally formed at domain walls of C-CDW-2 that are a consequence of any

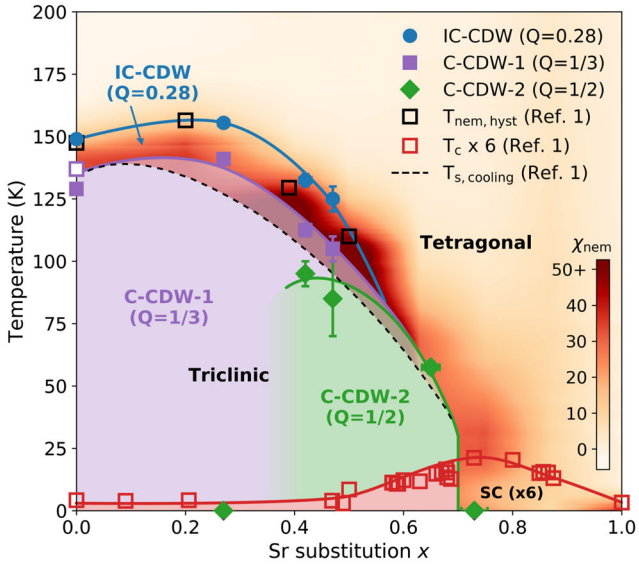

FIG. 5. Phase diagram of $Ba_{1-x}Sr_xNi_2As_2$ showing the IC-CDW (blue circles), C-CDW-1 (purple squares), and C-CDW-2 (green diamonds) phases. The hollow purple square at $x = 0$ represents the onset of the incipient CDW that undergoes a lock-in transition and evolves to C-CDW-1. The triclinic phase boundary on warming coincides with the boundary of C-CDW-1 and C-CDW-2. The overlaid color scale represents the nematic susceptibility, χ_{nem}. The onset of the strain hysteresis of the nematic response, $T_{\text{nem,hyst}}$ (black hollow squares), and the resistive superconducting T_c (red hollow squares) are shown together for comparison.

disorder present in the system. A system with a finite density of such defects would exhibit a thermodynamic transition to a uniform SC phase driven by Josephson coupling among nearby domain walls, albeit with a highly reduced T_c [29]. Thus, the onset of the resistive transition is where the CDW domain walls become superconducting, with macroscopic superconductivity being achieved at lower temperatures.

Another feature of the phase diagram (Fig. 5) is that there is a close correspondence between the presence of the IC-CDW and irreversible behavior in the nematic susceptibility measured with elastoresistance techniques [1]. When the IC-CDW is present, the strain response is hysteretic. As discussed above, it is possible that the IC-CDW couples strongly to the nematic order parameter, and therefore pins the nematic fluctuations. The hysteretic response then can be understood as the training of these static nematic domains by the applied elastic strain field. When the IC-CDW is absent, the nematic domains become dynamic, the response becomes reversible, and the fluctuations enhance superconductivity near $x_c = 0.7$, as claimed in Ref. [1].

Recently, Merz *et al.* [30] reported that $BaNi_2As_2$ is, in fact, orthorhombic in the IC-CDW phase. We see no evidence for such orthorhombicity in our study, though the magnitude of the orthorhombic distortion reported in Ref. [30] would be below our detection limit. The existence of such a phase could require a reinterpretation of the symmetry pattern of IC-CDW [Fig. 3(c)]. More detailed refinements of the crystal structure would shed light on this issue.

In summary, we showed that $Ba_{1-x}Sr_xNi_2As_2$ exhibits three distinct charge density waves, IC-CDW, C-CDW-1, and C-CDW-2. The order parameter of C-CDW-2, which is period-2, is always zero at antiphase domain walls, allowing the competing superconductivity to emerge locally. We also showed that the IC-CDW can strongly couple to the nematic order parameter, and promote static nematic domains by pinning the fluctuations. Our study establishes BSNA as a rare example of a material containing three distinct CDWs, and an exciting test bed for studying coupling between CDW, nematic, and SC orders.

We thank P. Ghaemi for an early collaboration, and S. A. Kivelson for discussions. X-ray experiments were supported by the U.S. Department of Energy, Office of Basic Energy Sciences Grant No. DE-FG02-06ER46285 (P. A.). Theory work was supported in part by the U.S. National Science Foundation Grant No. DMR 1725401 (E. F.). Materials synthesis was supported by the National Science Foundation Grant No. DMR1905891 (J. P.). P. A. and J. P. acknowledge the Gordon and Betty Moore Foundations EPiQS Initiative through Grants No. GBMF9452 and No. GBMF9071, respectively.

*abbamonte@mrl.illinois.edu

[1] C. Eckberg, D. J. Campbell, T. Metz, J. Collini, H. Hodovanets, T. Drye, P. Zavalij, M. H. Christensen, R. M. Fernandes, S. Lee, P. Abbamonte, J. W. Lynn, and J. Paglione, Nat. Phys. **16**, 346 (2020).
[2] S. Lee, G. de la Peña, S. X.-L. Sun, M. Mitrano, Y. Fang, H. Jang, J.-S. Lee, C. Eckberg, D. Campbell, J. Collini, J. Paglione, F. M. F. de Groot, and P. Abbamonte, Phys. Rev. Lett. **122**, 147601 (2019).
[3] E. Fradkin, S. A. Kivelson, and J. M. Tranquada, Rev. Mod. Phys. **87**, 457 (2015).
[4] J. M. Tranquada, Physica (Amsterdam) **460B**, 136 (2015).
[5] J. Paglione and R. L. Greene, Nat. Phys. **6**, 645 (2010).
[6] P. Dai, Rev. Mod. Phys. **87**, 855 (2015).
[7] P. Abbamonte, A. Rusydi, S. Smadici, G. D. Gu, G. A. Sawatzky, and D. L. Feng, Nat. Phys. **1**, 155 (2005).
[8] G. Ghiringhelli, M. Le Tacon, M. Minola, S. Blanco-Canosa, C. Mazzoli, N. B. Brookes, G. M. De Luca, A. Frano, D. G. Hawthorn, F. He, T. Loew, M. M. Sala, D. C. Peets, M. Salluzzo, E. Schierle, R. Sutarto, G. A. Sawatzky, E. Weschke, B. Keimer, and L. Braicovich, Science **337**, 821 (2012).
[9] R. Comin and A. Damascelli, Annu. Rev. Condens. Matter Phys. **7**, 369 (2016).
[10] J.-H. Chu, H.-H. Kuo, J. G. Analytis, and I. R. Fisher, Science **337**, 710 (2012).
[11] H.-H. Kuo, J.-H. Chu, J. C. Palmstrom, S. A. Kivelson, and I. R. Fisher, Science **352**, 958 (2016).

[12] C. Eckberg, L. Wang, H. Hodovanets, H. Kim, D. J. Campbell, P. Zavalij, P. Piccoli, and J. Paglione, Phys. Rev. B **97**, 224505 (2018).
[13] S. Lederer, E. Berg, and E.-A. Kim, Phys. Rev. Research **2**, 023122 (2020).
[14] W. L. McMillan, Phys. Rev. B **12**, 1187 (1975).
[15] See Supplemental Material at http://link.aps.org/supplemental/10.1103/PhysRevLett.127.027602 for the experimental details, the lattice parameters of samples and structural transitions, the symmetry patterns of CDWs, and for details of the theory, which includes Refs. [16–25].
[16] C. Chen, L. Su, A. H. Castro Neto, and V. M. Pereira, Phys. Rev. B **99**, 121108(R) (2019).
[17] W. L. McMillan, Phys. Rev. B **14**, 1496 (1976).
[18] T. Nattermann, in *Spin Glasses and Random Fields* (World Scientific, Singapore, 1998), pp. 277–298.
[19] L. D. Landau and E. M. Lifshitz, *Quantum Mechanics: Non-Relativistic Theory*, Course of Theoretical Physics Vol. v.3 (Butterworth-Heinemann, Oxford, 1991).
[20] Y. I. Joe, X. M. Chen, P. Ghaemi, K. D. Finkelstein, G. A. de la Peña, Y. Gan, J. C. T. Lee, S. Yuan, J. Geck, G. J. MacDougall, T. C. Chiang, S. L. Cooper, E. Fradkin, and P. Abbamonte, Nat. Phys. **10**, 421 (2014).
[21] J. E. Hoffman, E. W. Hudson, K. M. Lang, V. Madhavan, H. Eisaki, S. Uchida, and J. C. Davis, Science **295**, 466 (2002).
[22] S. A. Kivelson, D.-H. Lee, E. Fradkin, and V. Oganesyan, Phys. Rev. B **66**, 144516 (2002).
[23] Y. Yu and S. A. Kivelson, Phys. Rev. B **99**, 144513 (2019).
[24] B. Kalisky, J. R. Kirtley, J. G. Analytis, J.-H. Chu, A. Vailionis, I. R. Fisher, and K. A. Moler, Phys. Rev. B **81**, 184513 (2010).
[25] H. Xiao, T. Hu, A. P. Dioguardi, N. apRoberts Warren, A. C. Shockley, J. Crocker, D. M. Nisson, Z. Viskadourakis, X. Tee, I. Radulov, C. C. Almasan, N. J. Curro, and C. Panagopoulos, Phys. Rev. B **85**, 024530 (2012).
[26] A. S. Sefat, M. A. McGuire, R. Jin, B. C. Sales, D. Mandrus, F. Ronning, E. D. Bauer, and Y. Mozharivskyj, Phys. Rev. B **79**, 094508 (2009).
[27] J. Collini, S. Lee, S. X.-L. Sun, C. Eckberg, D. Campbell, J. Lynn, P. Abbamonte, and J. Paglione, arXiv:2106.12000.
[28] Y. Imry and S.-K. Ma, Phys. Rev. Lett. **35**, 1399 (1975).
[29] V. J. Emery, E. Fradkin, S. A. Kivelson, and T. C. Lubensky, Phys. Rev. Lett. **85**, 2160 (2000).
[30] M. Merz, L. Wang, T. Wolf, P. Nagel, C. Meingast, and S. Schuppler, arXiv:2012.05024.

Supplementary Information: Multiple charge density waves and superconductivity nucleation at antiphase domain walls in the nematic pnictide $Ba_{1-x}Sr_xNi_2As_2$

I. EXPERIMENTAL DETAILS

Single crystals of $Ba_{1-x}Sr_xNi_2As_2$ with $x = 0$, 0.27 ± 0.01, 0.42 ± 0.01, 0.47 ± 0.01, 0.65 ± 0.02, and 0.73 ± 0.02 were synthesized using the self-flux method reported in Ref. [1]. The precise chemical compositions were determined by energy dispersive x-ray spectroscopy on multiple spots on each sample. Single crystal x-ray scattering measurements were carried out using the in-lab x-ray instrument equipped with a Xenocs GeniX3D Mo K_α microspot x-ray source with multilayer focusing optics, providing 2.5×10^7 photons/sec in a beam spot of 130 μm at the sample position. The samples were cooled by a closed-cycle helium cryostat with a base temperature of 8 K mounted to a Huber four-circle diffractometer. The momentum resolution varied between $\Delta q = 0.01$ Å^{-1} and 0.08 Å^{-1} depending on the location in momentum space. Scattering signals were collected by a Mar345 image plate detector with 3450×3450 pixels. Three-dimensional surveys of momentum space were performed by taking images in 0.05° increments while sweeping samples through an angular range of 20° and mapping each pixel to the corresponding location in momentum space.

II. LATTICE PARAMETERS

Lattice parameters of $Ba_{1-x}Sr_xNi_2As_2$ samples in high-temperature tetragonal phase and low-temperature triclinic phase are determined using single crystal x-ray diffraction measurements with Mo K_α x-ray source (Table S1). The crystal structure of the low-temperature phase of $BaNi_2As_2$ is reported to be triclinic structure with $P\bar{1}$ symmetry by a previous structural refinement study in Ref. [2]. In this study, we used the standardized unit cell of the triclinic structure reported in Ref. [2]. Comparisons between the unit cell reported in Ref. [2] and the standardized unit cell can be found in the supplemental material of Ref. [3].

TABLE S1. Lattice parameters of $Ba_{1-x}Sr_xNi_2As_2$. Tetragonal lattice parameters are measured at room temperature and triclinic parameters at 50 K (except for $x = 0.42$, which is measured at 70 K).

	Tetragonal structure		Triclinic structure					
x	a (Å)	c (Å)	a (Å)	b (Å)	c (Å)	α (°)	β (°)	γ (°)
0	4.142(4)	11.650(3)	4.21(3)	3.99(2)	6.31(1)	105.2(3)	108.6(2)	89.3(4)
0.27	4.145(3)	11.499(3)	4.158(5)	4.155(6)	6.388(8)	108.2(1)	109.8(1)	89.2(2)
0.42	4.138(5)	11.271(3)	4.157(3)	4.13(1)	6.272(7)	108.5(2)	109.4(1)	89.7(1)
0.47	4.137(7)	11.211(5)	4.146(8)	4.10(2)	6.313(4)	109.12(7)	110.6(1)	89.2(2)
0.65	4.140(1)	10.928(3)	4.126(8)	4.06(3)	6.16(1)	109.6(2)	109.5(1)	89.8(1)
0.73	4.150(4)	10.812(5)	-	-	-	-	-	-

III. STRUCTURAL PHASE TRANSITION IN $Ba_{0.58}Sr_{0.42}Ni_2As_2$

The tetragonal-to-triclinic structural phase transition in $Ba_{0.58}Sr_{0.42}Ni_2As_2$ is summarized in Fig. S1. When cooled across the phase transition, the $(0, 1, 9)_{\text{tet}}$ structural Bragg reflection in the tetragonal phase splits into four reflections due to the formation of twin domains in triclinic phase [Fig. S1(a)]. One domain is chosen among the four, and the reflection of the domain is indexed as $(-1, 0, 5)_{\text{tri}}$. The line scans through $(0, 1, 9)_{\text{tet}}$ and $(-1, 0, 5)_{\text{tri}}$ show a sharp transition in their integrated intensity at $T_s = 112.5 \pm 2.5$ K, indicating the change in symmetry of crystal structure [Figs. S1(b), (c)]. At $T_{C2} = 95 \pm 5$ K, when C-CDW-2 forms, the magnitude of the triclinic distortion increases and the intensity of the triclinic Bragg reflection exhibits another sharp increase [Figs. S1(c)]. This indicates that C-CDW-2 has a cooperative relationship with the triclinic phase itself.

IV. SYMMETRY PATTERN OF IC-CDW

The IC-CDW exhibits a peculiar symmetry pattern that, in a given Brillouin zone (BZ), the satellite reflections appear only one direction, either along H or K direction. However the direction is not unique: the satellites appear at $(\pm 0.28, 0, 0)_{\rm tet}$ in some BZs, and at $(0, \pm 0.28, 0)_{\rm tet}$ in others. Fig. S2 shows the directionality of the IC-CDW in H-K maps at odd-numbered L in several different BZs measured in $Ba_{1-x}Sr_xNi_2As_2$, $x = 0$, 0.27, 0.42, 0.47. By combining the patterns shown in Fig. S2 together, and assuming that the BZ at $\boldsymbol{Q}$ has the same pattern as the BZ at $-\boldsymbol{Q}$, we obtained the symmetry pattern of the IC-CDW in H-K plane at odd-numbered L (Fig. 3 in the main text). Due to not enough data, we could not determine the symmetry pattern at even-numbered L.

V. UNIDIRECTIONALITY OF C-CDW-1 AND C-CDW-2

The satellite reflections of C-CDW-1 and C-CDW-2 appear in K direction, not in H direction, indicating that they are unidirectional. Fig. S3(a) shows the C-CDW-1 reflections in multiple Brillouin zones (BZs) at $(0, \pm 1/3, 0)_{\rm tri}$ and none is observed at $(\pm 1/3, 0, 0)_{\rm tri}$. Similarly, the C-CDW-2 reflections are observed at $(0, \pm 1/2, 0)_{\rm tri}$, not at $(\pm 1/2, 0, 0)_{\rm tri}$, in multiple BZs [Fig. S3(b)]. Thus, we conclude that the C-CDW-1 and C-CDW-2 are unidirectional, which is consistent with the fact that the underlying lattice is in triclinic phase, in which $C4$ symmetry is broken.

VI. THEORY OF SUPERCONDUCTIVITY ON PERIOD-2 CDW DOMAIN WALLS

In this section we present details of the Landau-Ginzburg theory of superconductivity induced on domain walls of a period-2 CDW. Since the experimentally observed period-2 CDW is manifestly unidirectional we will present a simple one-dimensional theory. This can be easily extended to more complex orders with several CDW ordering wave vectors.

Following the work of McMillan [4], we represent the CDW as a modulation of the local charge density $\rho(x)$ of the form

$$\rho(x) = \rho_0 + \psi(x)e^{iQx} + \psi^*(x)e^{-iQx} + \text{higher harmonics} \tag{1}$$

where ρ_0 is the average charge density and $\psi(x)$ is the (generally complex) CDW order parameter. However, in the period-2 case $Q = \pi$ (in units in which the lattice constant is set to unity), i.e. is a vector at the boundary of the Brillouin Zone. Hence, in this case the CDW order parameter is *real*, $\psi(x) = \psi^*(x)$, and it is slowly varying at the scale of the lattice spacing. We will also assume that there is a competing (also inhomogeneous) superconducting state represented by a local SC complex order parameter (the pairing amplitude) $\Delta(x)$ which, as we will see is not generally constant. We will be interested in the case in which the period-2 CDW is the "stronger order" and that it turns on at a higher temperature than the weaker SC order, $T_c^{\rm CDW} > T_c^{\rm SC}$. We will make use of gauge invariance of the SC order to work in the London gauge in which the SC order parameter is also real, $\Delta = \Delta^*$.

These assumptions lead us to the simplest possible form of the Landau-Ginzburg theory with competing CDW and SC orders whose free energy has the form

$$F = \int dx \left\{ \frac{K_{\rm CDW}}{2}(\partial_x\psi(x))^2 + \frac{r_{\rm CDW}}{2}\psi^2(x) + \frac{u_{\rm CDW}}{4}\psi^4(x) + \frac{K_{\rm SC}}{2}(\partial_x\Delta(x))^2 + \frac{r_{\rm SC}}{2}\Delta^2(x) + \frac{u_{\rm SC}}{4}\Delta^4(x) + \gamma\ \psi^2(x)\Delta^2(x) \right\} \tag{2}$$

Here $K_{\rm CDW}$ and $K_{\rm SC}$ are the stiffnesses of the CDW and the SC order parameters, respectively, and

$$r_{\rm CDW} = a_{\rm CDW}(T - T_c^{\rm CDW}), \qquad r_{\rm SC} = a_{\rm SC}(T - T_c^{\rm SC}) \tag{3}$$

We will assume that the coupling constants $u_{\rm CDW} > 0$ and $u_{\rm SC} > 0$, but we will allow the biquadratic coupling constant γ to have either sign (provided its magnitude is not too large). We will be interested in the regime in which the system is in the period-2 CDW phase but above the uniform SC state. Thus, $T_c^{\rm SC} < T < T_c^{\rm CDW}$, and in this regime $r_{\rm CDW} < 0$ and $r_{\rm SC} > 0$.

The free energy of Eq.(2) is in the simplest form that one can write, but one could also consider additional terms. For instance, in Ref.[5] Chen and coworkers considered a biquadratic term with two derivatives of the form $\mu\ \Delta^2(x)\ (\partial_x\psi(x))^2$. For $\mu < 0$ (and large enough) such a term can favor the spontaneous formation of CDW domain walls with local SC order. On the other hand, unless one thinks that this term is due to disorder (see below), the resulting CDW state will be weakly incommensurate, which is not what is seen (thus far) in the low temperature regime of the period-2 state of $Ba_{1-x}Sr_xNi_2As_2$. In addition, while it is true that these gradient terms can lead to

inhomogeneous states, it is difficult in practice to reach a regime in which $|\mu|$ is large enough (in virtue of the gradient coupling form of this term). We should note that if the CDW order has a period other than 2, its order parameter is complex and, in this case, the natural topological defects of the CDW are *discommensurations* at which the *phase* of its order parameter changes by 2π, while the amplitude remains unchanged [6]. Thus, in the case of a commensurate CDW with a wave vector not at the boundary of the Brillouin Zone the scheme that we consider here is not operative but it can be achieved again if one considers a large enough gradient coupling. Finally, we are also not including other interesting physical effects such as the presence of a metallic component which can lead to interesting temperature dependences of the ordering wave vector, among other things.

Here we will assume that the domain walls are due to the presence of disorder. Indeed, impurities generate local random potentials $V_{\rm dis}(x)$ which couple linearly to the local charge density $\rho(x)$ and hence also couple linearly to the CDW order parameter. Since in the period-2 case the order parameter is real, this coupling is analogous to the problem of a uniaxial ferromagnet (and Ising model) coupled to a local random field. A general argument by Imry and Ma [7] shows that a random field destroys long-range order in the 2D Ising model (and in any dimension below 4 for the incommensurate case) driven by the proliferation of domain walls. In three dimensions, in the commensurate case the domain walls proliferate only if the disorder is strong enough and there is a phase transition between the ordered and the disordered state (for a review see Ref. [8]). On the other hand, in a layered system the 2D to 3D crossover leads to a broad fluctuational regime. Pnictides are anisotropic but not layered so they are regarded as an intermediate case in which nevertheless these fluctuations are significant particularly in doped systems. The upshot of this analysis is that in the period-2 CDW phase of $Ba_{1-x}Sr_xNi_2As_2$ one expects a significant number of antiphase domain walls.

We will now show that domain walls of $Ba_{1-x}Sr_xNi_2As_2$ are actually superconducting. For simplicity we will consider a unidirectional period-2 CDW with a single domain wall. To this effect let us consider the Landau-Ginzburg equations for the free energy of Eq.(2). They are

$$-K_{\rm CDW}\partial_x^2\psi(x)+r_{\rm CDW}\psi(x)+u_{\rm CDW}\psi^3(x)+\gamma\psi(x)\Delta^2(x)=0, \tag{4}$$

$$-K_{\rm SC}\partial_x^2\Delta(x)+r_{\rm SC}\Delta(x)+u_{\rm SC}\Delta^3(x)+\gamma\psi^2(x)\Delta(x)=0 \tag{5}$$

In the regime $r_{\rm CDW}<0$ we will look for solutions with $\psi\neq 0$ and $\Delta(x)\neq 0$ satisfying the boundary conditions

$$\lim_{x\to\pm\infty}\psi(x)=\pm\psi_0, \qquad \lim_{x\to\pm\infty}\Delta(x)=0 \tag{6}$$

where $\psi_0=\sqrt{|r_{\rm CDW}|/u_{\rm CDW}}$ is the value of the period-2 CDW order parameter in the absence of the wall; in this regime, $r_{\rm SC}>0$, there is no uniform superconductivity and $\Delta=\Delta_0=0$.

We will consider the simpler case in which the stiffnesses of the CDW and the SC order parameters are the same, i.e. $K_{\rm CDW}=K_{\rm SC}\equiv K$. Furthermore, we will also require the quartic and biquadratic coupling constants to satisfy $u_{\rm CDW}=u_{\rm SC}=2\gamma\equiv u$, by which these couplings become $\frac{u}{4}(\psi^2+\Delta^2)^2$. With these assumptions the free energy of Eq.(2) simplifies,

$$F=\int dx\,\Big[\frac{K}{2}[(\partial_x\psi)^2+(\partial_x\Delta)^2]+\frac{1}{2}(r_{\rm CDW}\psi^2+r_{\rm SC}\Delta^2)+\frac{u}{4}(\psi^2+\Delta^2)^2\Big] \tag{7}$$

Next, we define the two-component real field

$$\boldsymbol{n}(x)=(\psi(x),\Delta(x))=\psi_0(\cos\theta,\sin\theta) \tag{8}$$

where we used the fact that in the regime of interest the CDW order is dominant. Here we will be interested in the case in which $0\leq\theta\leq\pi$, which means that ψ takes values between $\pm\psi_0$. The free energy now becomes

$$F=\int dx\Big[\frac{\kappa}{2}(\partial_x\theta)^2-h\cos 2\theta+\varepsilon_0\Big] \tag{9}$$

where we used the following expressions for the effective stiffness κ, the anisotropy coupling constant h, and the uniform free energy density ε_0

$$\kappa\equiv K\psi_0^2=-\frac{K}{2u}(r_{\rm CDW}+r_{\rm SC})>0, \qquad h\equiv\frac{1}{8u}(r_{\rm CDW}^2-r_{\rm SC}^2)>0, \qquad \varepsilon_0\equiv-\frac{(r_{\rm CDW}+r_{\rm SC}))^2}{4u} \tag{10}$$

where we used that $r_{\rm CDW}<0$ and $|r_{\rm CDW}|>r_{\rm SC}>0$, and that in the uniform equilibrium broken symmetry state

$$\psi_0^2=-\frac{(r_{\rm CDW}+r_{\rm SC})}{u}>0 \tag{11}$$

The Landau-Ginzburg equation for the simplified free energy of Eq.(9) is

$$-\kappa\partial_x^2\theta + 2h\sin 2\theta = 0 \tag{12}$$

which, for $h > 0$ (dominant CDW) has the uniform solutions $\theta = 0, \pi$ corresponding to $\psi = \pm\psi_0$, respectively (and no superconductivity).

There is, however, a non-trivial domain wall solution of Eq.(12) which interpolates between these two uniform states. To find the solution we use the standard analogy by which we will regard the coordinate x as "time". In this picture Eq.(12) is regarded as the equation of motion of a "physical pendulum" whose degree of freedom is the angle θ. The "energy" of the pendulum is

$$E = \frac{\kappa}{2}(\partial_x\theta)^2 + h\cos 2\theta \tag{13}$$

The energy of the pendulum for the uniform solutions $\theta = 0, \pi$ is just h. There is another solution also with energy h which satisfies

$$\frac{\kappa}{2}(\partial_x\theta)^2 + h\cos 2\theta = h \tag{14}$$

or, what is the same as

$$(\partial_x\theta)^2 = 2\frac{h}{\kappa}(1 - \cos 2\theta) \tag{15}$$

This is equivalent to the first order differential equations

$$\partial_x\theta = \pm 2\sqrt{\frac{h}{\kappa}}\sin\theta \tag{16}$$

The solutions to this first order differential equation are

$$\theta_\pm(x) = 2\tan^{-1}\left(e^{\pm 4\sqrt{\frac{h}{\kappa}}x}\right) \tag{17}$$

where we set the arbitrary origin at $x = 0$, where $\theta_\pm(0) = \frac{\pi}{2}$. After some algebra we find that the domain wall solutions for the CDW and SC order parameters are

$$\psi(x) = \pm\psi_0\tanh\left(4\sqrt{\frac{h}{\kappa}}x\right), \qquad \Delta(x) = \frac{\psi_0}{\cosh\left(4\sqrt{\frac{h}{\kappa}}x\right)} \tag{18}$$

Clearly, the solution with positive sign interpolates between $\theta = \pi$, i.e. $\psi \to -\psi_0$ as $x \to -\infty$, and $\theta = 0$, i.e. $\psi \to +\psi_0$ as $x \to +\infty$. This solution describes the domain wall (the solution with the negative sign describes the anti-domain wall). It is apparent that far from the domain wall the CDW order parameter becomes $\pm\psi_0$ and approaches these values exponentially fast. Conversely, the SC order parameter Δ vanishes exponentially fast far from the domain wall and reaches its maximum value, ψ_0 within our simplifications, at the location of the topological defect. The free energy cost of the domain wall per unit length (or area) of the wall is the difference of the free energy of Eq.(9) for these solutions relative to the uniform state and is given by $F_{\rm wall} = 2\sqrt{h\kappa} > 0$.

In this derivation we assumed that $\gamma = 2u$ which means that the biquadratic term is as important as the usual quartic terms. However, solutions of this type can be obtained in the more general case in which γ is weak. In that case one can first find a CDW domain wall solution and then solve for the SC state nucleated at the wall (assuming that the back reaction is parametrically small). Since $T_{\rm CDW}^c \gg T_{\rm SC}^c$, we can find an approximate domain wall solution of Eqs.(4) and (5) that satisfy the domain wall boundary conditions, Eq.(6), by assuming that the coupling constant γ in Eq.(4) is weak and then solve Eq.(5) in the background of the CDW domain wall. With this approximation, the solution to Eq.(4) that obeys the boundary condition of Eq.(6) is (centered arbitrarily at $x = 0$)

$$\psi(x) = \psi_0\tanh(x/\xi_{\rm CDW}) \tag{19}$$

where $\xi_{\rm CDW} = |2K_{\rm CDW}/r_{\rm CDW}|^{1/2} \propto (T_c^{\rm CDW} - T)^{-1/2}$ is the CDW correlation length and $\psi_0 = \sqrt{|r_{\rm CDW}|/u_{\rm CDW}}$ is the expectation value in the uniform unperturbed CDW state.

Eq.(5) in the background of the CDW domain wall, which now becomes

$$-K_{\rm SC}\partial_x^2\Delta(x) + r_{\rm SC}\Delta(x) + \gamma\psi_0^2(x)\tanh^2(x/\xi_{\rm CDW})\,\Delta(x) + u_{\rm SC}\Delta^3(x) = 0 \tag{20}$$

We will seek a solution with $\Delta(x) \neq 0$ with lower free energy than the domain wall without SC order. The SC order parameter $\Delta(x)$ will be vanishingly small near the onset of the SC state. In this regime we can look for solutions of the *linearized* equation with an arbitrary amplitude

$$-K_{\rm SC}\partial_x^2\Delta(x) + r_{\rm SC}\Delta(x) + \gamma\psi_0^2(x)\tanh^2(x/\xi_{\rm CDW})\ \Delta(x) = 0 \tag{21}$$

and then fix the value of the amplitude by demanding that the free energy is minimized (including the non-linear term). Upon defining a rescaled coordinate $v = x/\xi_{\rm CDW}$, we can bring the linearized equation to the form of a Schrödinger equation of the form

$$-\frac{1}{2}\partial_v^2\Delta(u) + U(v)\Delta(v) = E\Delta(v) \tag{22}$$

where we defined

$$U(v) \equiv -\frac{\lambda(\lambda+1)}{2}\frac{1}{\cosh^2 v}, \tag{23}$$

$$E \equiv -\frac{r_{\rm SC}+\gamma\psi_0^2}{2K_{\rm SC}}\ \xi_{\rm CDW}^2 \tag{24}$$

where $\lambda(\lambda+1) = \gamma\psi_0^2/K_{\rm SC}$.

Eq.(22) is the Schrödinger equation for a stationary state with energy E in the Pöschl-Teller potential (given in Eq.(23)) [9]. The solutions are the Legendre functions $P_\lambda^\mu(v)$ where $E = -\mu^2/2$. This equation has a bound state with $E = -1/2$ and the solution is

$$\Delta(x) = \frac{A}{\cosh(x/\xi_{\rm CDW})} \tag{25}$$

where A is a constant to be determined. The important feature of this solution is that it vanishes (exponentially fast) as $x \to \pm\infty$.

Using the expression for the induced SC order parameter, Eq.(25), we find that the free energy of the SC state localized on the domain wall is

$$F_{\rm SC} = \frac{2K_{\rm SC}}{\xi_{\rm CDW}}\Big[-\frac{1}{2} + \frac{(r_{\rm SC}+\gamma\psi_0^2)}{2K_{\rm SC}}\Big]\ A^2 + \frac{1}{3}\xi_{\rm SC}u_{\rm SC}\ A^4 \tag{26}$$

The SC state localized on the domain wall becomes favorable if the quantity in brackets in Eq.(26) becomes negative, or, what is the same as $E = -1/2$. Upon minimizing Eq.(26) we find that the amplitude A is given by

$$A^2 = -\frac{3K_{\rm SC}}{u_{\rm SC}\xi_{\rm CDW}}\Big[-\frac{1}{2} + \frac{(r_{\rm SC}+\gamma\psi_0^2)}{2K_{\rm SC}}\Big] > 0 \tag{27}$$

It is apparent that solutions that we found in the regime $\gamma \ll u$, Eqs. (19) and (25), have the same form as in the regime $\gamma = 2u$ discussed above, Eq.(18), albeit with somewhat different parameters. There is, however, an important difference in this regime. By inspection we see that there is a critical temperature for the SC solution on the wall to exist, given by the condition that the quantity in brackets in Eq.(27) vanishes. This temperature is much lower than the critical temperature of the period 2 CDW state.

On the other hand, since the free energy of the SC wall solution is not zero, these topological defects of the CDW state cannot be formed spontaneously in the period 2 CDW ordered phase. However, disorder can (and does) favor the creation of domain walls. We noted in the text that disorder coupes to the period 2 CDW in the same way as a random field in an Ising ferromagnet. A standard argument due to Imry and Ma [7] shows that in two dimensions *any* amount of random field disorder destroys the long range ordered state, the period 2 CDW in this case, while in higher dimensions a critical amount of disorder is needed. In layered systems there is an intermediate broad fluctuational regime signaling the 2D to 3D crossover. However, while $Ba_{0.58}Sr_{0.42}Ni_2As_2$ is anisotropic, the anisotropy is not large enough to regard this system (as well as all pnictides) as being layered (in contrast with the cuprate superconductors).

We should note that it is reasonable to expect that doping could drive $Ba_{1-x}Sr_xNi_2As_2$ weakly incommensurate by creation of domain walls (as in the McMillan scenario [6]). A similar mechanism was previously proposed in $TiSe_2$ [10], which also exhibits a period-2 CDW (see also Ref. [5]). The incommensuration of the CDW in $TiSe_2$ arises because the domain walls form a periodic structure [10]. The result is a tiny shift of the CDW Bragg peak from the commensurate position. This shift is, however, very small, $\sim 10^{-3}$ r.l.u.. Such a small shift would not be visible in our current measurements, which were carried out on a lab-based x-ray source whose resolution is 20 times lower

than that used in Ref. [10]. We therefore cannot make any statement about whether a slight incommensurate shift is present also in the C-CDW-2 phase of $Ba_{1-x}Sr_xNi_2As_2$. Note, however, that our argument about domain wall superconductivity does not require the domain walls to be ordered. Randomly distributed domain walls could also lead to a heterogeneous superconducting state, though would not result in a coherent shift of the peak. Nevertheless, a precision measurement of the commensurability of IC-CDW-2, analogous to Ref. [10], would be an important subject of a future study.

We make an additional remark on previous experimental results on the doping evolution of T_c. In Eckberg et al. [1], the authors claim that the superconducting T_c near the critical composition $x_c = 0.7$ is enhanced by nematic fluctuations due to a quantum phase transition. This enhancement takes place on both sides of the phase boundary, so the resistive transition is observed to be ~ 3 K both for x just above and below x_c. Because of the presence of C-CDW-2 at $0.4 < x < x_c$, the thermodynamic signature of superconductivity is suppressed to 0.5 K, where global phase coherence is established. Although this T_c of 0.5 K may seem to be similar to that for $x \leq 0.4$, there is no requirement, in our picture, that this temperature be the same as the resistive transition for $x < 0.4$, where no nematic enhancement takes place. For $x < 0.4$ where only C-CDW-1 is present, the order parameter of C-CDW-1 is complex since it is period-3, and thus C-CDW-1 does not lead to the same suppression of the thermodynamic T_c. Our arguments about domain wall superconductivity apply only to a period-2 CDW, whose order parameter is real.

Therefore, we conclude that a SC state will be nucleated at the antiphase domain walls of the period 2 CDW. We can regard this phenomenon as the onset of local superconductivity. However the thermodynamic transition to a macroscopic superconducting state will only happen at a substantially lower temperature driven by the Josephson coupling between nearby domain walls (see, e.g. Ref. [11]). We should note that this phenomenon bears a close analogy with the CDW order seen in the SC halos of vortices of high T_c superconductors [12, 13], cuprate superconductors in high magnetic fields [14], and iron-based superconductors with structural twin domains [15] or antiferromagnetic domains [16].

[1] C. Eckberg, D. J. Campbell, T. Metz, J. Collini, H. Hodovanets, T. Drye, P. Zavalij, M. H. Christensen, R. M. Fernandes, S. Lee, P. Abbamonte, J. W. Lynn, and J. Paglione, Sixfold enhancement of superconductivity in a tunable electronic nematic system, Nature Physics **16**, 346 (2020).

[2] A. S. Sefat, M. A. McGuire, R. Jin, B. C. Sales, D. Mandrus, F. Ronning, E. D. Bauer, and Y. Mozharivskyj, Structure and anisotropic properties of $Ba_{1-x}Sr_xNi_2As_2$ single crystals, Phys. Rev. B **79**, 094508 (2009).

[3] S. Lee, G. de la Peña, S. X.-L. Sun, M. Mitrano, Y. Fang, H. Jang, J.-S. Lee, C. Eckberg, D. Campbell, J. Collini, J. Paglione, F. M. F. de Groot, and P. Abbamonte, Unconventional Charge Density Wave Order in the Pnictide Superconductor $Ba_{1-x}Sr_xNi_2As_2$, Phys. Rev. Lett. **122**, 147601 (2019).

[4] W. L. McMillan, Landau theory of charge density waves in transition-metal dichalcogenides, Phys. Rev. B **12**, 1187 (1975).

[5] C. Chen, L. Su, A. H. Castro Neto, and V. M. Pereira, Discommensuration-driven superconductivity in the charge density wave phases of transition-metal dichalcogenides, Phys. Rev. B **99**, 121108 (2019).

[6] W. L. McMillan, Theory of discommensurations and the commensurate-incommensurate charge-density-wave phase transition, Phys. Rev. B **14**, 1496 (1976).

[7] Y. Imry and S.-K. Ma, Random-Field Instability of the Ordered State of Continuous Symmetry, Phys. Rev. Lett. **35**, 1399 (1975).

[8] T. Nattermann, Theory of the Random Field Ising Model, in *Spin Glasses and Random Fields*, edited by A. P. Young (World Scientific, Singapore, 1998) pp. 277–298, arXiv:cond-mat/9705295.

[9] L. D. Landau and E. M. Lifshitz, *Quantum Mechanics: Non-Relativistic Theory*, third, revised and enlarged ed., Course of Theoretical Physics, Vol. v.3 (Butterworth-Heinemann, Oxford, 1991).

[10] Y. I. Joe, X. M. Chen, P. Ghaemi, K. D. Finkelstein, G. A. de la Peña, Y. Gan, J. C. T. Lee, S. Yuan, J. Geck, G. J. MacDougall, T. C. Chiang, S. L. Cooper, E. Fradkin, and P. Abbamonte, Emergence of charge density wave domain walls above the superconducting dome in 1T-$TiSe_2$, Nature Physics **10**, 421 (2014).

[11] V. J. Emery, E. Fradkin, S. A. Kivelson, and T. C. Lubensky, Quantum Theory of the Smectic Metal State in Stripe Phases, Phys. Rev. Lett. **85**, 2160 (2000).

[12] J. E. Hoffman, E. W. Hudson, K. M. Lang, V. Madhavan, H. Eisaki, S. Uchida, and J. C. Davis, A four unit cell periodic pattern of quasi-particle states surrounding vortex cores in $Bi_2Sr_2CaCu_2O_{8+\delta}$., Science **295**, 466 (2002).

[13] S. A. Kivelson, D.-H. Lee, E. Fradkin, and V. Oganesyan, Competing order in the mixed state of high-temperature superconductors, Phys. Rev. B **66**, 144516 (2002).

[14] Y. Yu and S. A. Kivelson, Fragile superconductivity in the presence of weakly disordered charge density waves, Phys. Rev. B **99**, 144513 (2019).

[15] B. Kalisky, J. R. Kirtley, J. G. Analytis, J.-H. Chu, A. Vailionis, I. R. Fisher, and K. A. Moler, Stripes of increased diamagnetic susceptibility in underdoped superconducting $Ba(Fe_{1-x}Co_x)_2as_2$ single crystals: Evidence for an enhanced superfluid density at twin boundaries, Phys. Rev. B **81**, 184513 (2010).

[16] H. Xiao, T. Hu, A. P. Dioguardi, N. apRoberts Warren, A. C. Shockley, J. Crocker, D. M. Nisson, Z. Viskadourakis, X. Tee,

I. Radulov, C. C. Almasan, N. J. Curro, and C. Panagopoulos, Evidence for filamentary superconductivity nucleated at antiphase domain walls in antiferromagnetic $CaFe_2As_2$, Phys. Rev. B **85**, 024530 (2012).

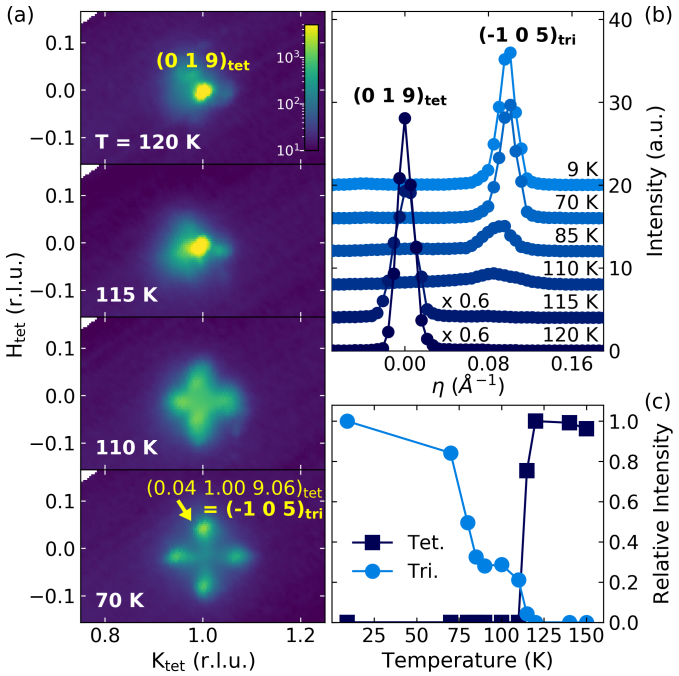

FIG. S1. Tetragonal-to-triclinic structural phase transition in $Ba_{0.58}Sr_{0.42}Ni_2As_2$. (a) H-K maps at a selection of temperatures showing the evolution of $(0, 1, 9)_{\rm tet}$ structural Bragg reflection across the phase transition. The splitting of the reflection below $T = T_{\rm s}$ is due to the formation of twin domains in triclinic phase. (b) Line momentum scans through tetragonal $(0, 1, 9)_{\rm tet}$ and triclinic $(-1, 0, 5)_{\rm tri}$ Bragg reflections. η is the distance in momentum space from $(0, 1, 9)_{\rm tet}$ along the direction to $(-1, 0, 5)_{\rm tri}$. (c) Integrated intensities of the tetragonal (Tet.) and triclinic (Tri.) Bragg reflections, showing the change in symmetry of crystal structure at $T = T_{\rm s}$. Another sharp increase of the intensity of the triclinic Bragg reflection at the onset of C-CDW-2, at $T_{\rm C2} = 95 \pm 5$ K, indicates a cooperative relationship between C-CDW-2 and the triclinic phase.

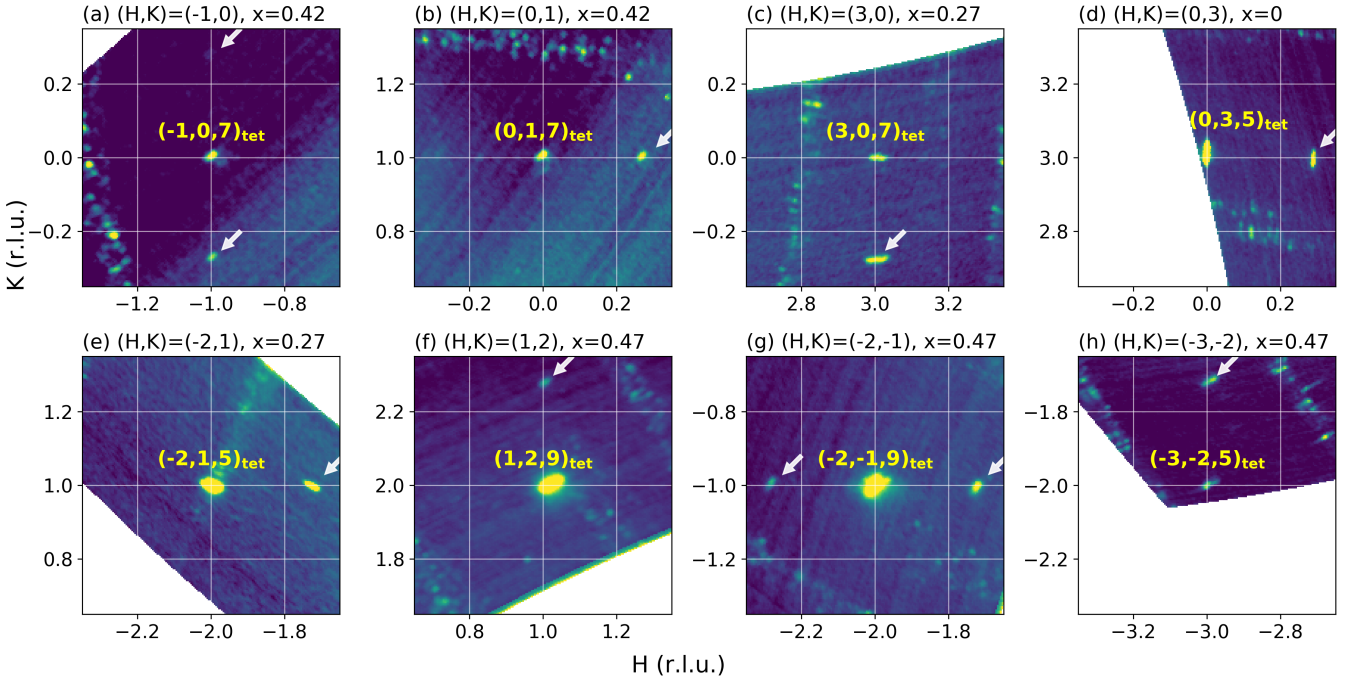

FIG. S2. Selected H-K maps at odd-numbered L of IC-CDW in several different Brillouin zones measured in $Ba_{1-x}Sr_xNi_2As_2$, $x = 0$, 0.27, 0.42, 0.47. The IC-CDW satellite reflections are indicated with white arrows. The indices of Brillouin zones and the Sr content x are labeled in each panel.

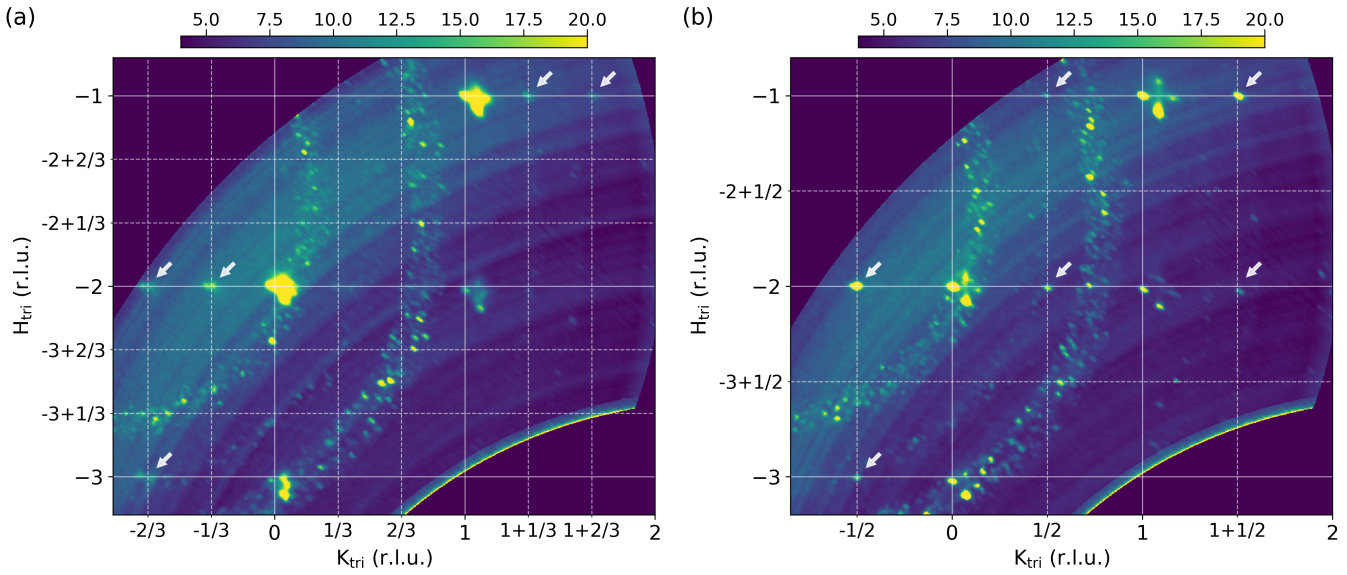

FIG. S3. (a) H-K map at $L_{\rm tri} = 6$ of $Ba_{0.58}Sr_{0.42}Ni_2As_2$ at $T = 110$ K. C-CDW-1 satellite reflections appear at $(0, \pm 1/3, 0)_{\rm tri}$ (white arrows), not at $(\pm 1/3, 0, 0)_{\rm tri}$. (b) Similar map at $T = 9$ K, showing C-CDW-2 reflections at $(0, \pm 1/2, 0)_{\rm tri}$ (white arrows), not at $(\pm 1/2, 0, 0)_{\rm tri}$.